I J C T A, 9(38), 2016, pp. 239-251

The Acting Effects on the System Response Time for Three Types of Nanofluids, Carbon Nanoparticle-based-water, Metal Nanoparticles-water and Metal Oxide Nanoparticles-water

Mefteh Bouhalleb* and Hassen Abbassi**

ABSTRACT

Finite-Element Method, with the SIMPLER algorithm of pressure-velocity coupling is applied to investigate the natural convection flow utilizing nanofluids in square enclosure with a sinusoidal heated wall. The fluid in the cavity is a water based nanofluid containing different types of nanoparticles: copper (Cu), silver (Ag), gold (Au), carbon nanotube (CNT), alumina (Al_2O_3),titania (TiO_2), Zinc Oxide (ZnO), copper oxide (CuO). The influence of the Rayleigh number (between 10^3 and 10^5) and solid volume fraction of nanoparticle (between 0 and 0.1) on the fluid flow and heat transfer are numerically investigated.The main objective of this work is to make a comparison between the heat transfer performance of the metallic oxide nanoparticle suspended in water, metallic particles suspended in water and carbon nanoparticle-based suspension in water.

Keywords: Nanofluid, heat transfer performance, finite-element method, etc.

1. INTRODUCTION

Nanofluids have become a topic of interest for improving heat transfer performance related to energy savings. Therefore, researchers have been investigating the various thermophysical properties of nanofluids. These fundamental properties need to be investigated before studying the heat transfer performance of nanofluids, because the performance measurements such as heat transfer, energy, exergy etc. depend on these fundamental properties.

Based on the available studies on the fundamental properties of nanofluids, it is found that, thermal conductivity [1, 2], viscosity [3, 4] and density [5, 6] augment accordingly with the enhancement of volume concentration. Furthermore, thermal conductivity increases with the increase of temperature [7, 8]. However, viscosity and density decreases with the increase of temperatures [5, 9, 10]. Since the overall properties of the nanofluids are better than conventional fluids therefore, there are strong opportunity to increase the overall performance of the heat exchangers by using nanofluids as working fluids and energy losses can be reduced all over the world. Shahrul et al. [11, 12] performed analytical study with a shell and tube heat exchanger considering various oxide based nanofluids at different mass flow rates. They analyzed 0.01–0.04 volume fractions of ZnO, CuO, Fe3O4, TiO2, and Al2O3 nanoparticles into the water. Energy effectiveness improvement was found to be approximately 23–52% for the above-listed nanofluids. In their study, highest energy effectiveness has been obtained for ZnO–W nanofluid and lowest found for SiO2–W nanofluid.

*,** Unit of Computational Fluid Dynamics and Transfer Phenomena, National Engineering School of Sfax, Tunisia, *Email: meftehbouhalleb@gmail.com*

** Faculty of Sciences of Sfax, Department of Physics, BP 1171, 3000 Sfax-University of Sfax, Tunisia

Gupta et al.[13], by experimental evaluation of graphene nanofluid thermal conductivity, demonstrated that nanofluid causes increase in thermal conductivity even in low volume fractions. This thermal conductivity will improve by increase of volume fraction. Primoz Ternik [14] examined the effect of adding Au nanoparticles to Newtonian base fluid on the conduction and convection heat transfer characteristics in a differentially heated cubic enclosure. The numerical results show that Variation of the mean Nusselt number is marginally affected by the increase of the volume fraction of nanoparticles for a given set of values of the nanofluid Rayleigh number.

I.M. Shahrul et al have experimentally investigated the performance of a shell and tube heat exchanger operated with Al2O3–water, SiO2–water, and ZnO–water nanofluids. Numerical results show that approximately, 50%, 15%, and 9% enhancement of heat transfer coefficient were observed accordingly using the nanofluids ZnO–water, Al2O3–water, and SiO2–water, respectively compared to water.

Eastman et al.[15] used transient hot wire method to measure the thermal conductivity of Cu nanoparticle of mean diameter<10 nm in ethylene glycol. They found that the effective thermal conductivity increased by up to 40% with approximately 0.3% volumetric concentration of Cu nanoparticles over the base fluid. Keblinski et al.[16] studied the mechanism of heat transfer in nanofluids by considering Brownian motion, liquid/particle interface and the effect of nanoparticles clustering. They drew conclusions that Brownian motion was too slow to transport significant amount of heat, so thermal conductivity enhancements was due to a highly conductive layered structure around the particles and also due to cluster of particles separated by liquid layers thin enough to allow rapid heat flow among particles. Farajollahi et al. [17] investigated heat transfer of Al2O3-water and TiO2-water nanofluids in a shell and tube heat exchanger, experimentally. They used the mentioned nanofluids at 0.3, 0.5, 0.75, 1 and 2% volume concentration of nanoparticles in their experiments. They reported 19-56% and 18-56% enhancement in convective heat transfer of Al2O3-water and TiO2-water nanofluids compared with distilled water, respectively. Ray et al. [18] studied nanofluid performance in a compact minichannel plate heat exchanger experimentally and numerically. They used Al2O3, CuO and SiO2 nanoparticles suspended in ethylene glycol and water mixture as nanofluid. Their reports showed that, convective heat transfer coefficient and overall heat transfer coefficient increase for each of the three types of nanofluids. Hdz-García et al. [19] formed nanofluids by lubricating oil and 1–100 nm nanoparticles. Currently, common nanoparticles mainly include metal nanoparticles (Cu, Ag, etc.), oxide nanoparticles (Al2O3, SiO2, CuO, etc.), and MoS2 nanoparticles, as well as single-walled, double-walled, and multi-walled carbon nanotubes (CNTs). Each nanoparticle has distinct molecular structural and chemical characteristics. Thus, different nanofluids have varying impacts on lubrication and heat transfer performance. CNTs with large molecular length-diameter ratio have considerably higher heat conductivity coefficient than other nanoparticles. In Tiwari's experiments [20], done for a wide range of nanoparticle volume concentrations and coolant flow rates, various nanofluids had different optimum volume concentrations in which heat transfer characteristics showed a maximum enhancement. Among the nanofluids tested at optimum volume concentration, CeO2-water nanofluids obtained the highest overall heat transfer coefficient ratio, followed by Al2O3-water, TiO2-water, and, finally, SiO2-water. For CeO2-water, Al2O3-water, TiO2-water, and SiO2-water nanofluids, the maximum heat transfer coefficient enhancements at optimum volume concentration were about 35.9%, 26.3%, 24.1%, and 13.9%. Furthermore, by using thermal conductivity of 3 different nanofluids, including aluminum oxide, copper oxide, and titanium oxide, Hojjat et al.[21] have proven that thermal conductivity is a function of fluid temperature, nanofluid volume fraction, and nanoparticle thermal conductivity. Their presented model showed a very good match compared to experimental method which led to more accuracy in comparison with Hamilton model, which was not capable of evaluating base fluid temperature influence and also the amount of volume fraction.

In a numerical study, Haddad et al. [22] investigated the natural convection of a nanofluid in the Rayleigh–Benard cell with and without the effect of Brownian motion and thermophoresis. Without considering these two effects, heat transfer rate decreased. When these two effects were considered the heat transfer

rate increased as a result of induction of a slip velocity between the base fluid and the nanoparticles. Some recent control papers are discussed in [32-35].

The objective of the present study is to examine the best nanofluid for maximum heat transfer as well as for performance index and comparison within various nanofluids. Effects of various operating parameters (volume fraction of nanoparticles, Rayleigh number, etc.) on the flow structure and response time are discussed as well.

2. STATEMENT OF THE PROBLEM

The geometry of the present problem is shown in fig 1. It displays a two dimensional square cavity with the size of L = 0.04m. A sinusoidal temperature is imposed along the left vertical wall (T_C + a.sin(πt/Θ), while the vertical right wall is cooled at a constant temperature T_c. The top and bottom horizontal walls have been considered to be adiabatic. The nanofluid is Newtonian and incompressible. The flow is considered to be steady, two dimensional and laminar, and the radiation effects are negligible. The base fluid and the nanoparticles are in thermal equilibrium. Thermophysical properties of water and nanoparticles are assumed to be constant and are given in table 1. The thermo physical properties of the nanofluid are assumed constant except for the water density variation, which is determined based on the Boussinesq approximation.

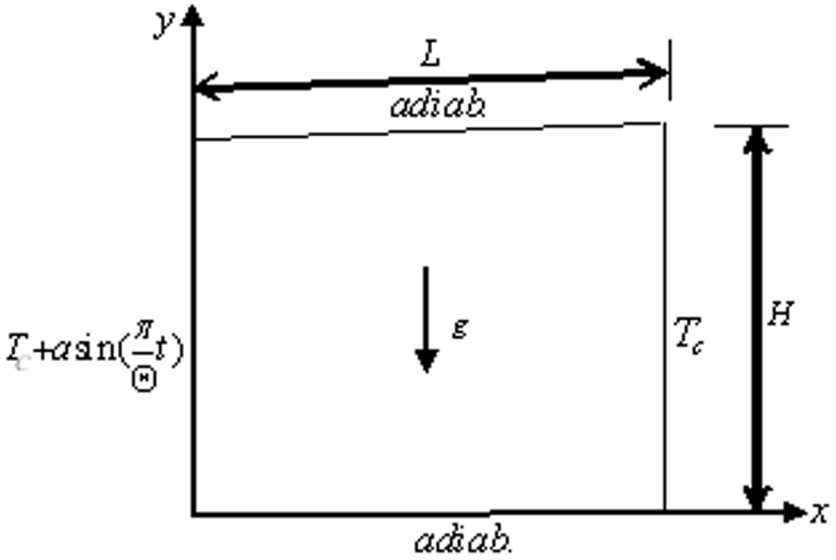

Figure 1: Studied problem with boundary conditions and coordinate system

Table 1
Physical properties of pure water and solid particles.

$\rho C_p k \beta$	(kgm^{-3})	($Jkg^{-1}K^{-1}$)	($Wm^{-1}K^{-1}$)	(k^{-1})
Pure water	997.1	4179	0.613	2.1×10^{-4}
Cu	6320	531.8	76.5	1.8×10^{-5}
O Al_2O_3	3880	765	40	0.8×10^{-5}
ZnO	5600	519.3	15	0.65×10^{-5}
TiO_2	4250	686.5	8.95	0.9×10^{-5}
CNT	1350	3500	1350	4.2×10^{-5}
Cu	8933	385.00	429.00	1.89×10^{-5}
Ag	10500	235	429.00	1.89×10^{-5}
Au	19320	128.8	314.4	1.416×10^{-7}

3. MATHEMATICAL FORMULATION

By the law of mass conservation, momentum and energy, the governing equations are:

$$\frac{\partial u}{\partial x}+\frac{\partial v}{\partial y}=0 \tag{1}$$

$$\frac{\partial u}{\partial \tau}+u\frac{\partial u}{\partial x}+v\frac{\partial u}{\partial y}=-\frac{\partial p}{\partial x}+\frac{\mu_{nf}}{\rho_{nf}\alpha_f}\left(\left(\frac{\partial^2 u}{\partial x^2}+\frac{\partial^2 u}{\partial y^2}\right)\right)+\frac{(\rho\beta)_{nf}}{\rho_{nf}\beta_f}Ra\,\mathrm{Pr}\,\theta\sin\omega \tag{2}$$

$$\frac{\partial v}{\partial \tau}+v\frac{\partial v}{\partial x}+v\frac{\partial v}{\partial y}=-\frac{\partial p}{\partial y}+\frac{\mu_{nf}}{\rho_{nf}\alpha_f}\left(\left(\frac{\partial^2 v}{\partial x^2}+\frac{\partial^2 v}{\partial y^2}\right)\right)+\frac{(\rho\beta)_{nf}}{\rho_{nf}\beta_f}Ra\,\mathrm{Pr}\,\theta\cos\omega \tag{3}$$

$$\frac{\partial \theta}{\partial \tau}+u\frac{\partial \theta}{\partial x}+v\frac{\partial \theta}{\partial y}=\frac{\alpha_{nf}}{\alpha_f}\left(\frac{\partial^2 \theta}{\partial x^2}+\frac{\partial^2 \theta}{\partial y^2}\right) \tag{4}$$

The boundary conditions are as follow:

On all solid boundaries: $u = 0$ $v = 0$

On $x = 0,\ 0 \le y \le 1 : \theta = a.\sin(\pi\tau/\Theta)$ (5)

On $x = 1,\ 0 \le y \le 1 : \theta = 0$

On y = 0 and 1, $0 \le x \le 1 : \dfrac{\partial \theta}{\partial y}=0$

The expressions of density, specific heat, thermal expansion coefficient and dynamic viscosity of the nanofluid are given as follows [23]:

$$\rho_{nf}=(1-\phi)\rho_f+\phi\rho_s \tag{6}$$

$$(\rho C_p)_{nf}=(1-\phi)(\rho C_p)_f+\phi(\rho C_p)_s \tag{7}$$

$$(\rho\beta)_{nf}=(1-\phi)(\rho\beta)_f+\phi(\rho\beta)_s \tag{8}$$

$$\mu_{nf}=\frac{\mu_f}{(1-\phi)^{2.5}} \tag{9}$$

The local Nusselt number *Nu(x)* can be expressed as:

$$Nu(y)=-\frac{k_{eff}}{k_f}\left(\frac{\partial \theta}{\partial x}\right)_{x=1} \tag{10}$$

Effective conductivity k_{eff} of the nanofluid is calculated as follows [24]:

$$k_{eff}=k_{stat}+k_{brow}$$

The static conductivity k_{stat} is given by the Maxwell model [25]model:

$$k_{stat}=k_f\frac{k_s+2k_f+2(k_s-k_f)\phi}{k_s+2k_f-(k_s-k_f)\phi} \tag{11}$$

Vajjha and Das [26] improved the model of Koo and Kleinstreuer [24] by deriving a new equation for β_1 and *f(T, φ)* using their own experimental data.

$$f(T,\varphi) = \left(2.8217\times10^{-2}\varphi + 3.917\times10^{-3}\right)\frac{T}{T_0} + \left(-3.0669\times10^{-2}\varphi - 3.91123\times10^{-3}\right) \tag{12}$$

The brownian conductivity is formulated as (Koo and Kleinstreuer[24]):

$$k_{brow} = 5\times10^4\,\beta_1\phi\rho_f C_{pf}\sqrt{\frac{\kappa T}{\rho_s d_s}}\,f(T,\phi) \tag{13}$$

Where ρ_s and d_s are the density and the diameter of nanoparticles, respectively and k is the Boltzmann constant $k = 1.3807 \times 10^{-23}$ *J/K* and T_0 is the reference temperature equal to 273K. β_1 listed in table 2 for different nanofluids.

The total heat transferred from the hot wall to the flow is evaluated by the space averaged Nusselt number expressed as:

$$Nu = \frac{1}{Ar}\int_0^{Ar} Nu(y)\,dy \tag{14}$$

Table 2
Curve-fit relations for new fraction of the liquid volume, β_1

Type of particles	β_1	*concentration*	*Temperature*
CuO, Cu, Ag	$9.881(100\varphi)^{-0.9446}$	$1\% \le \varphi \le 6\%$	$298K \le T \le 363K$
Al_2O_3	$8.4407(100\varphi)^{-1.07304}$	$1\% \le \varphi \le 10\%$	$298K \le T \le 363K$
ZnO	$8.4407(100\varphi)^{-1.07304}$	$1\% \le \varphi \le 10\%$	$298K \le T \le 363K$

4. NUMERICAL METHODOLOGY

A modified version of Control Volume Finite-Element Method (CVFEM) of Saabas and Baliga [27] is adapted to the standard staggered grid in which pressure and velocity components are stored at different points. The SIMPLER algorithm of Patankar [28] was applied to resolve the pressure-velocity coupling in conjunction with an Alternating Direction Implicit (ADI) scheme for performing the time evolution. The numerical code used here is described and validated in details in Abbassi et al. [29,30].The necessary conditions to prevent numerical instabilities are determined from a combination of Courant–Friedrichs–Lewy (CFL) conditions and the restrictions on the grid Fourier number. According to the CFL conditions, the distance travelled by the fluid in one time increment must be less than one space increment (Δx or Δy), and lead to a constraint on the time step Δτ:

$$\Delta\tau \prec \left\{\frac{\Delta x}{u};\frac{\Delta y}{v}\right\} \tag{15}$$

From this condition, the used grid and velocity fields, the time step is limited by $\Delta\tau \prec 1.57\times10^{-4}$. In the following computations Δτ is fixed at 10^{-5}.

5. GRID REFINEMENT AND TEST VALIDATION

Grid refinement tests have been performed for four uniform grids: 51×51, 61×61, 71×71 and 81×81 for $Ra = 10^5$, φ = 4% and Ar =1 applied to configuration of our problem. Results show that when we moved

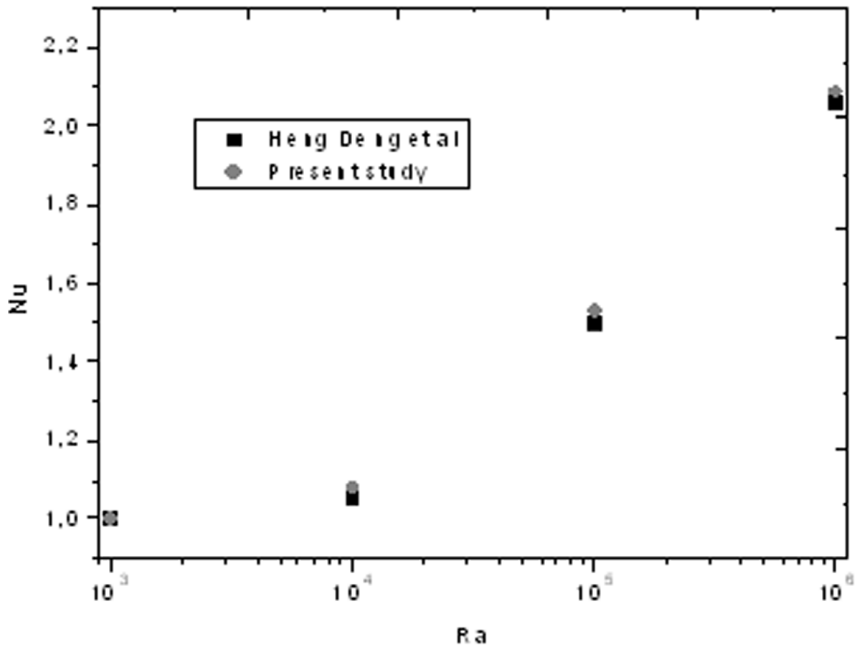

Figure 2: Test validation: Comparisons with Qi-Hang Deng and Juan-Juan Chang [31] with *Pr* = 0.71 and *Ar* = 1.

from the first grid to the second, the Nusselt number *Nu* moved from 3.1447 to 3.1185, undergoing a variation of 0.84%. When we moved from the second grid to the third, the Nusselt number becomes 3.1030, undergoing a decrease of 0.50%. Now, when we moved from the third grid to the fourth, the Nusselt number becomes 3.0952, undergoing a decrease of only 0.25%. We conclude that the grid of 71×71 is sufficient to carry out the numerical study of this flow. A particular care is taken when varying the aspect ratio; the grid is extended or reduced keeping constant space steps.

The present code was also tested to simulate the case studied by Qi-Hong Deng and Juan-Juan Chang [31]. We calculated average Nusselt number for the rectangular enclosure with sinusoidal space temperature distributions on the left side wall at Pr = 0.71 and for various Rayleigh numbers. As can be seen from fig. 2, the results predicted by current computer code agree well with the previous study.

6. RESULTS AND DISCUSSION

Effect of metal nanoparticles on the heat transfer

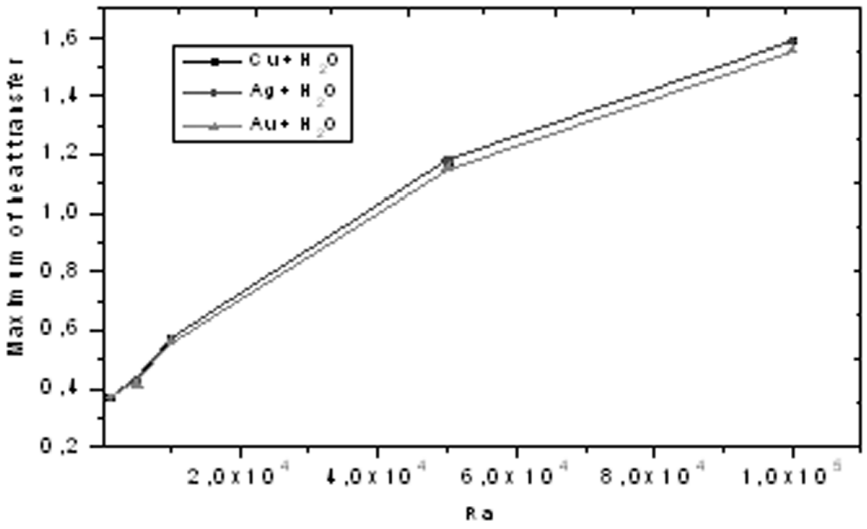

Figure 3: Effects of Rayleigh number for the different metal nanoparticles.

Effects of Rayleigh number for different types of metal nanoparticles is shown in fig.3. We note that the nanofluid with copper (Cu) and silver (Ag) show a better heat transfer performance than the nanofluid with the (Au) nanoparticles.

6.1. Effect of metal oxide nanoparticles on the heat transfer

The influence of Rayleigh number for different types of metal oxide nanoparticles is shown in fig.4. Fig.4 shows that the curves of four metal oxide nanoparticles used in this work are close to each other. But the nanofluid with nanopaticules Al2O3 remains the best heat conductor, among other nanoparticles (CuO, ZnO and TiO2). In this study, highest energy effectiveness has been obtained for Al2O3–water nanofluid and lowest found for TiO2–water nanofluid.

According to the authors, the key factor is the fact that Al2O3 nanoparticles formed relatively small clusters when compared to the other nanoparticles (CuO, ZnO and TiO2).

6.2. Comparison between different types of nanoparticles

Effects of Rayleigh number for different types of nanoparticles (carbon nanoparticles, metal nanoparticles and metal oxide nanoparticles) on the heat transfer (Nusselt number) for $\varphi = 4\%$ is shown in figure 5. It can

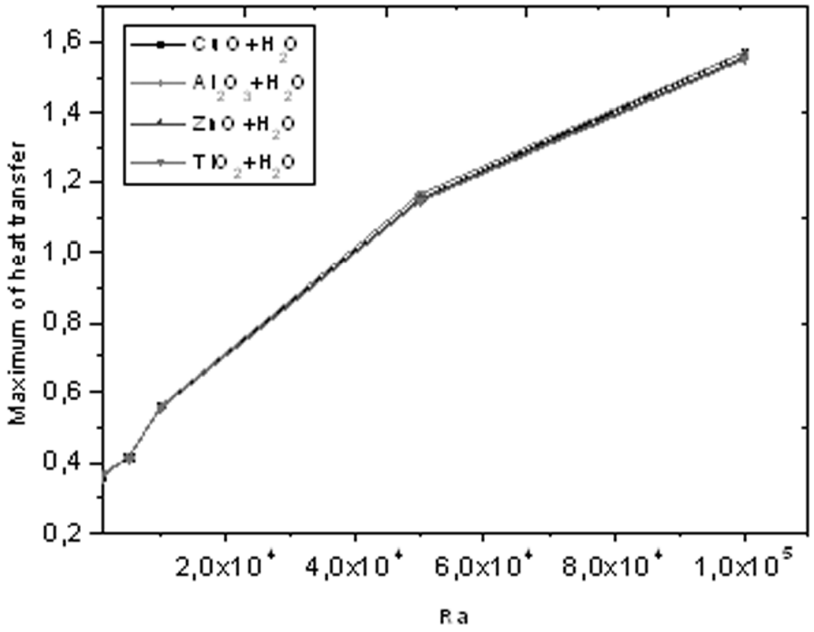

Figure 4: Effects of Rayleigh number for the different metal oxide nanopaticles.

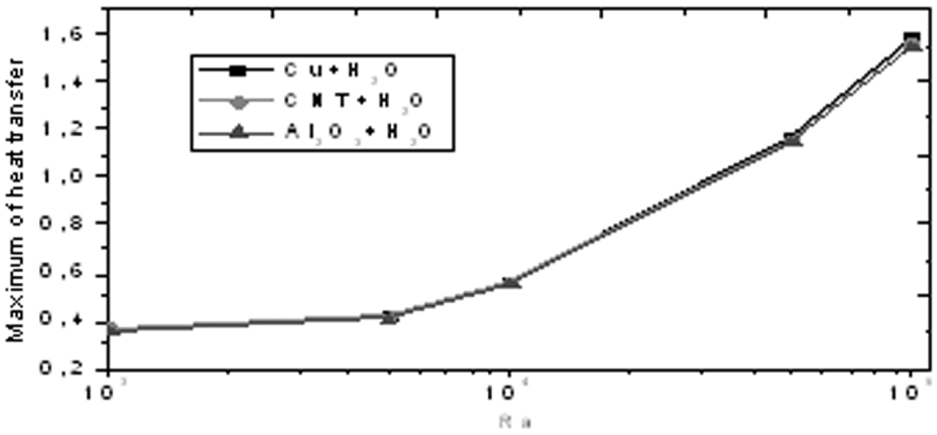

Figure 5: Effects of Rayleigh number for the different types of nanopaticles.

be that heat transfer change by using different types of nanofluid. This means that the nanofluids have a great effect on the heating processes. Choosing copper as the nanoparticle leads to the maximumamounts of Nusselt number, while minimum amounts of them are obtained by using alumina. Also, it is found that the difference among different types of nanofluid enhancement becomes more pronounced at high Rayleigh number (Ra>=104).

All the above-mentioned data indicate that choosing copper leads to highest heating performance for this problem.

6.3. Influence of Brownian effects on heat transfer

Figure 6 shows the time evolution of the average Nusselt number (Nu) with Brownian effect and without Brownian effect for Cu+water nanofluid. At the beginning, Nu is typically zero, indicating that heat does not reach the right wall; therefore the system begins to respond after a finite time delay. After this time the Nusselt number will go up very quickly, it reaches a maximum value and then, gradually decreases.

According to Figure 6, the Brownian effect is then at the origin of the important increase in heat transfer for weak solid volume fraction. In a suspension, the nanoparticles move randomly and thus cause the movement of a relatively large volume of liquid surrounding them. This microscale interaction can occur between the hot and cold regions, which increases the heat flux.

6.4. Influence of nanoparticles volume fraction on heat transfer

Figure 7 shows the variation of heat transfer as a function of heating time, for three nanoparticles volume concentrations φ = 0%, 1% and 6%. As show in this figure, the system begins to respond after a finite time, these the necessary time so that the heat reaches the cold wall. The figure zoom, represents the response time of system for different nanoparticles volume fraction.

Variation of time response with particle volume fraction of the studied nanofluid (Cu-water) shows that, with the increasing volume fraction of nanoparticles, the time response of system decreases. That is to

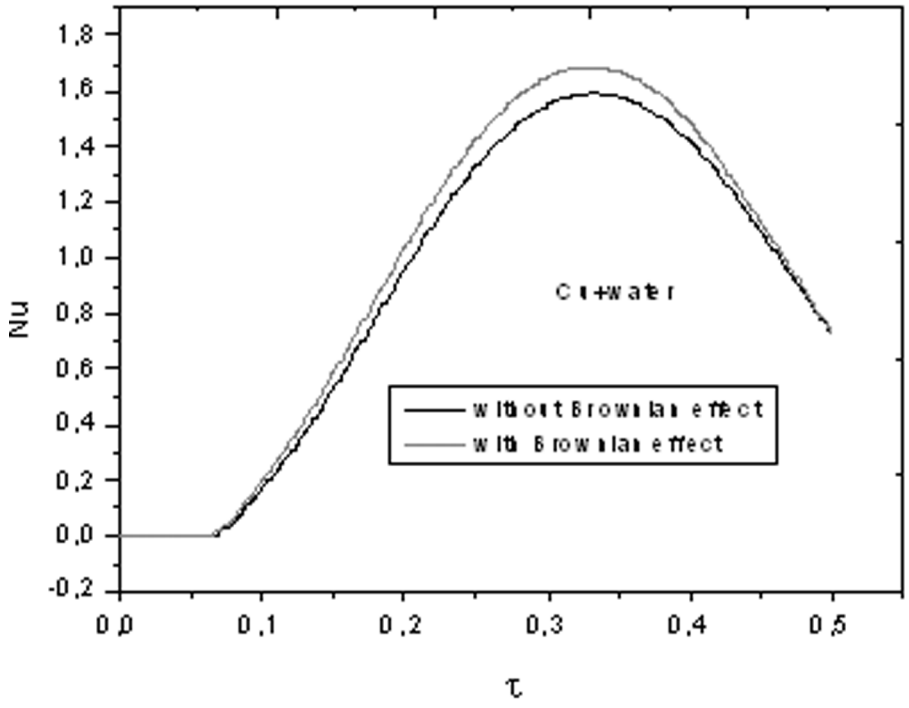

Figure 6: Evolution of Nusselt number with time for Cu + water nanofluid with $Ra = 10^5$ and φ =1%.

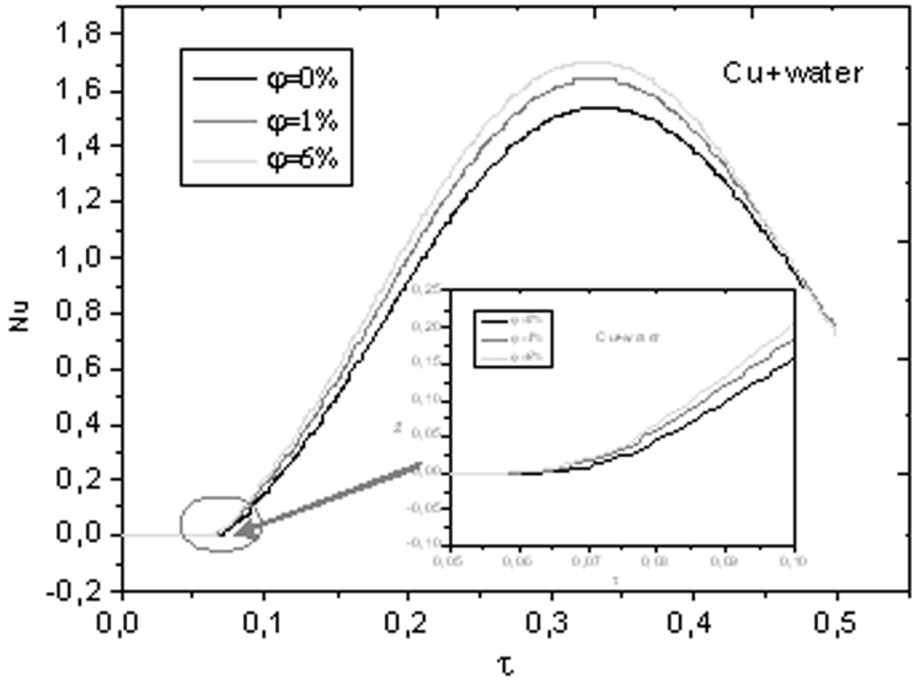

Figure 7: Evolution of Nusselt number a function of time for different nanoparticles volume fractionWith $Ra=10^5$.

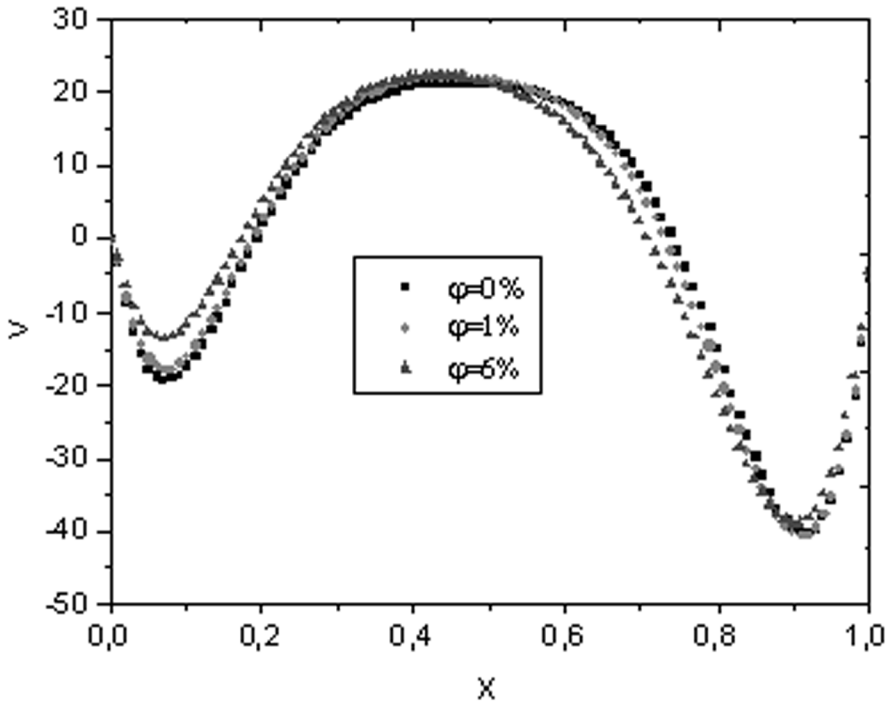

Figure 8: Horizontal velocity at (x, y = 0.5) for various concentration of nanoparticles with $Ra=10^5$ and $\tau = \Theta$.

say that the time required for the heat to pass from the hot wall to the cold wall, decreases. For example when the concentration of nanoparticles increases from 0% to 6%, the decrease of response time reached 18%.

After a half period the Nusselt number reached a maximum. We note that the maximum of the Nusselt number increases with increase of the nanoparticles volume fraction.

For example when the concentration of nanosolids increases from 0% to 6%, the increase of amplitude reached 10%.

The addition of solid particles into base fluid plays a double role; it augments the effective conductivity of the mixture causing heat transfer enhancement but also augments the viscosity of the nanofluid leading to the damping of flow motion, as shown in Figure 8, then causing a low increase in heat transfer, when the concentration of nanoparticles reached 6%.

6.5. Influence of Rayleigh number on heat transfer

The variation of Nusselt number with time for two Rayleigh number (Ra = 104 and Ra = 105) is displayed in figure 9.

We notice that after excitation by a sinusoidal temperature, the response time (ôresp) of the system decreases by decreasing the Rayleigh number. For Ra = 104 the heat transfer occurs by pure conduction, so the ratio of heat transfer is equal to the ratio of thermal conductivities, hence the low amplitude of Nusselt number. For Ra = 105, the onset of the convective heat transfer regime, and the amplitude of Nusselt number shows a significant increase. This observation is the consequence of the important thermal dispersion.

6.6. Influence of Rayleigh number on the flow structure

Streamline (left) and isotherm (right) for different Rayleigh numbers when φ = 4%, (Cu–Water case) are depicted in Figure 10. A singular cell is formed at low Rayleigh number and the shape of the main celliscircular (Figure 10 (a)). As shown in Figure 10(b–c), the cell carries the same form but tends towards the cold wall for Ra = 104 and eventually the shape of the cell has a tendency to break up into two vortices for Ra = 105. We note that for Ra = 105 the flow field is dominated by a primary large cell filling most of the cavity rotating in a clockwise direction, then, it appears a weak small secondary cell rotating in the counter clockwise direction. Isotherms are concentrated in the vicinity of the hot wall for Ra = 103, moves to the cold wall and forms a boundary layer at the active walls for Ra = 104. At Ra = 105 the temperature field occupies the totality of the enclosure, and the maximum of thermal dispersion is very close to the vertical walls.

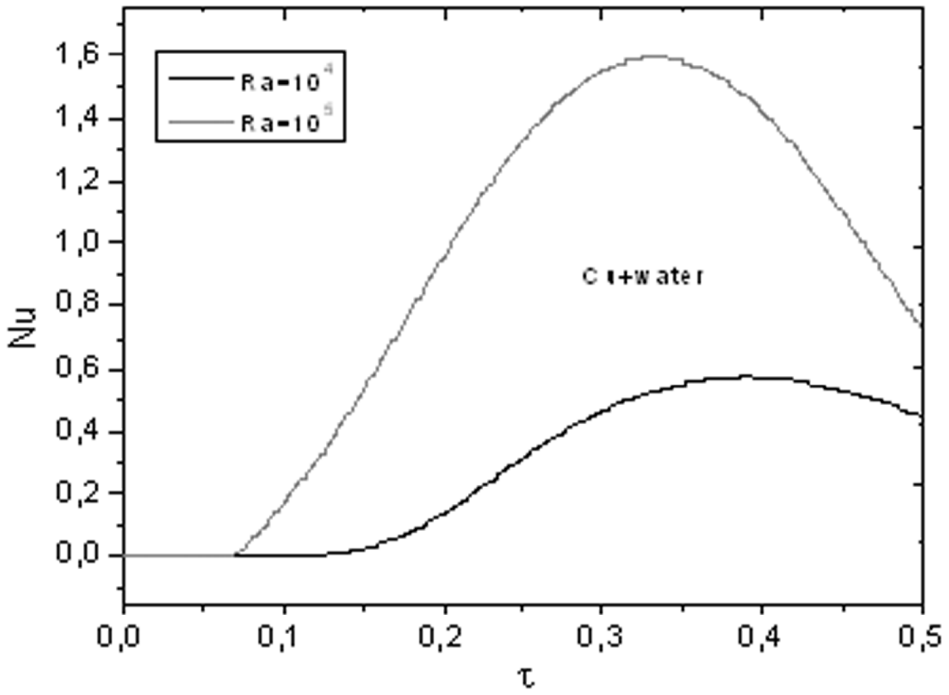

Figure 9: Evolution of Nusselt number a function of time for different Rayleigh number with φ = 4%.

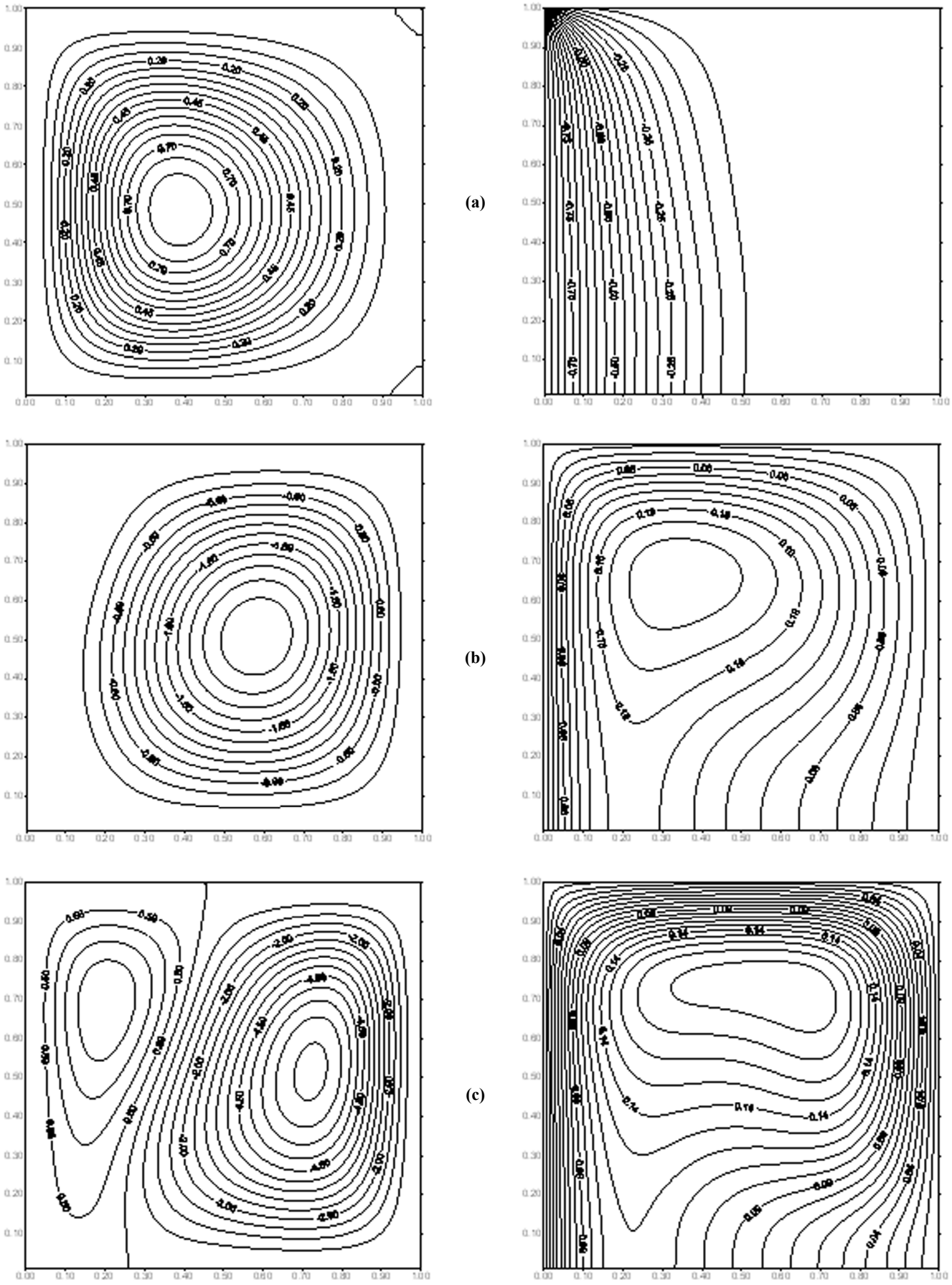

Figure 10 Streamline (left) and isotherm (right) for (a) $Ra = 10^3$,(b)$Ra = 10^4$ and (c) $Ra = 10^5$ when $\varphi = 4\%$ (Cu–Water case).

7. CONCLUSION

In the present study, steady and laminar natural convection in square cavity using nanofluid is investigated numerically. The enclosure is partially heated and other two opposite walls are adiabatic.Effects of nanoparticle volume fraction, types of nanofluid and Rayleigh numbers on the flow and heat transfer characteristics have been examined. The type of nanofluid is a key factor for heat transfer enhancement. The highest values are obtained when using copper nanoparticle. Increase in the Rayleigh number leads to response time decrease. The increase of Rayleigh number from 104 to 105, leads to a change in the structure of the flow.

REFERENCES

[1] S.M.S. Murshed, K.C. Leong and C. Yang, "Investigations of thermal conductivity and viscosity of nanofluids,"*International Journal of Thermal Sciences,* **47** (5), 560-568, 2008.

[2] K.C. Leong, C. Yang, S.M.S. Murshed, "A model for the thermal conductivity of nanofluids – the effect of interfacial layer,"*Journal of Nanoparticle Research*, **8** (2), 245-254, 2006.

[3] I.M. Mahbubul, R. Saidur, M.A. Amalina, "Latest developments on the viscosity of nanofluids,"*International Journal of Heat and Mass Transfer*, **55** (4), 877-888, 2012.

[4] C.T. Nguyen, F. Desgranges, N. Galanis, G. Roy, T. Mare, S. Boucher and H.Angue Mintsa, "Viscosity data for Al_2O_3–water nanofluid—hysteresis: is heat transfer enhancement using nanofluids reliable?", *International Journal of Thermal Sciences,* **47** (2), 103-111, 2008.

[5] M.M. Elias, I.M. Mahbubul, R. Saidur, M.R. Sohel, I.M. Shahrul, S.S.Khaleduzzaman and S. Sadeghipour, "Experimental investigation on the thermophysical properties of Al_2O_3 nanoparticles suspended in car radiator coolant,"*International Communications in Heat and Mass Transfer,* **54**, 48-53,2014.

[6] I.M. Mahbubul, R. Saidur and M.A. Amalina, "Thermal conductivity, viscosity and density of R141b refrigerant based nanofluid,"*Procedia Engineering*, **56**, 310–315, 2013.

[7] I.M. Mahbubul, R. Saidu and M.A. Amalina, "Influence of particle concentration and temperature on thermal conductivity and viscosity of Al_2O_3/R141b nanorefrigerant,"*International Communications in Heat and Mass Transfer*, **43**,100–104, 2013.

[8] W. Duangthongsuk and S. Wongwises, "Measurement of temperature-dependent thermal conductivity and viscosity of TiO_2–water nanofluids,"*Experimental Thermal and Fluid Science*, **33** (4), 706-714, 2009.

[9] R.S. Vajjha and D.K. Das, A review and analysis on influence of temperature and concentration of nanofluids on thermophysical properties, heat transfer and pumping power, *International Journal of Mass and Heat Transfer*, **55**, 4063-4078, 2012.

[10] I.M. Mahbubul, I.M. Shahrul, S.S. Khaleduzzaman, R. Saidur, M.A. Amalina and A.Turgut, "Experimental investigation on effect of ultrasonication duration on colloidal dispersion and thermophysical properties of alumina–water nanofluid,"*International Journal of Mass and Heat Transfer*, **88**, 73-81, 2015.

[11] I.M. Shahrul, I.M. Mahbubul, R. Saidur, S.S. Khaleduzzaman, M.F.M. Sabri, M.M. Rahman, Effectiveness study of a shell and tube heat exchanger operated with nanofluids at different mass flow rates, Numer. Heat Transfer Part A: Appl, 2014, 65 (7), 699–713.

[12] I.M. Shahrul, I.M. Mahbubul, R. Saidur, M.F.M. Sabri and S.S. Khaleduzzaman, "Energy and environmental effects of shell and tube heat exchanger by using nanofluid as a coolant,"*Journal of Chemical Engineering of Japan*, **47** (4), 340, 344, 2014.

[13] S.S. Gupta, V.M. Siva, S. Krishnan, T.S. Sreeprasad, P.K. Singh, T. Pradeep and S.K. Das, "Thermal conductivity enhancement of nanofluids containing graphene nanosheets,"*Journal of Applied Physics*, **110**, Article ID 084302, 2011.

[14] P. Ternik, "Conduction and convection heat transfer characteristics of water–Au nanofluid in a cubic enclosure with differentially heated side walls,"*International Journal of Heat and Mass Transfer*, **80**, 368-375, 2015.

[15] J.A. Eastman, S.U.S. Choi, S. Li, W. Yu and L.J. Thompson, "Anomalously increased effective thermal conductivities of ethylene glycol-based nanofluids containing copper nanoparticles,"*Applied Physics Letters*, **78** (6), 718-720, 2001.

[16] P. Keblinski, S.R. Phillot, S.U.S. Choi and J.A. Eastman, "Mechanisms of heat flow in suspensions of nano-sized particles (nanofluids)," *International Journal of Heat and Mass Transfer*, **45**, 855-863, 2002.

[17] B. Farajollahi, S. Gh. Etemad and M. Hojjat, "Heat transfer of nanofluids in a shell and tube heat exchanger,"*International Journal of Heat and Mass Transfer*, **53**, 12-17, 2010.

[18] D.R. Ray, D.K. Das and R.S. Vajjha, "Experimental and numerical investigations of nanofluids performance in a compact minichannel plate heat exchanger,"*International Journal of Heat and Mass Transfer*, **71**, 732-746, 2014.

[19] H.M. Hdz-García, M.I. Pech-Canul, R. Muñoz-Arroyo, A.I. Mtz-Enriquez, J.L. Acevedo-Dávila, M.J. Castro-Román and F.A. Reyes-Valdés, "304 Stainless steel brazing incorporating tungsten nanoparticles,"*Journal of Materials Processing Technology*, **215**, 1-5, 2015.

[20] A.K. Tiwari, P. Ghosh and J. Sarkar, "Performance comparison of the plate heat exchanger using different nanofluids,"*Experimental Thermal and Fluid Science*,**49**, 141-151, 2013.

[21] M. Hojjat, S.Gh. Etemad, R. Bagheri and J. Thibault,"Thermal conductivity of non-Newtonian nanofluids: experimental data and modeling using neural network,"*International Journal of Heat and Mass Transfer*, **54** (5), 1017-1023, 2011.

[22] Z. Haddad, E. Abu-Nada, H.F. Oztop and A. Mataoui, "Natural convection in nanofluids: are the thermophoresis and Brownian motion effects significant in nanofluid heat transfer enhancement?",*International Journal of Thermal Sciences*, 57, 152-162, 2012.

[23] B. Ghasmi and S.M. Aminossadati, "Natural convection heat transfer in an inclined enclosure filled with a water-CuO nanofluid," *Numerical Heat Transfer: Part A*,**55**, 807-823, 2009.

[24] J. Koo and C. Kleinstreuer, "A new thermal conductivity model for nanofluids," *Journal of Nanoparticle Research*, **6** (6), 577–588, 2004.

[25] J. Maxwell, *A Ttreatise on Electricity and Magnetism*, University Press, Oxford, U.K., 1904.

[26] R.S. Vajjha and D.K. Das, "Experimental determination of thermal conductivity of three nanoûuids and development of new correlations,"*International Journal of Heat and Mass Transfer*, **52**, 4675-4682, 2009.

[27] H.J. Saabas and B.R. Baliga, "Co-located equal-order control-volume ûnite-element method for multidimensional incompressible, ûuid ûow part I: formulation,"*Numerical Heat Transfer: Part B*, **26** (4), 381-407, 1994.

[28] S.V. Patankar, *Numerical Heat Transfer and Fluid Flow*, CRC Press, Boca Raton, FL, USA, 1980.

[29] H. Abbassi, S. Turki and S. Ben Nassrallah, "Interpolation functions in control volume finite element method," *Computational Mechanics*, **30**, 303-309,2003.

[30] H. Abbassi, S. Turki and S. Ben Nassrallah, "Numerical investigation of forced convection in a plane channel with a built-in triangular prism,"*International Journal of Thermal Sciences*, **40**, 649-658, 2001.

[31] Q.H. Deng and J.J Chang, "Natural Convection in a Rectangular Enclosure with Sinusoidal Temperature Distributions on Both Side Walls,"*Numerical Heat Transfer A*, **54**, 507-524, 2008.

[32] S. Vaidyanathan, K. Madhavan and B.A. Idowu, "Backstepping control design for the adaptive stabilization and synchronization of the Pandey jerk chaotic system with unknown parameters", *International Journal of Control Theory and Applications*, **9** (1), 299-319, 2016.

[33] S. Vaidyanathan and A. Boulkroune, "A novel hyperchaotic system with two quadratic nonlinearities, its analysis and synchronization via integral sliding mode control," *International Journal of Control Theory and Applications*, **9**(1), 321-337, 2016.

[34] S. Sampath, S. Vaidyanathan and V.T. Pham, "A novel 4-D hyperchaotic system with three quadratic nonlinearities, its adaptive control and circuit simulation*," International Journal of Control Theory and Applications*, **9** (1), 339-356, 2016.

[35] S. Vaidyanathan and S. Sampath, "Anti-synchronization of identical chaotic systems via novel sliding control method with application to Vaidyanathan-Madhavan chaotic system," *International Journal of Control Theory and Applications*, **9** (1), 85-100, 2016.